LAWRENCE
LIVERMORE
NATIONAL
LABORATORY

LLNL-TR-659075

Plutonium Adsorption and Desorption from Bentonite: Progress Report FT-14LL0807071

J. D. Begg, M. Zavarin, S. J. Tumey, A. B. Kersting

August 20, 2014

Disclaimer

This work performed under the auspices of the U.S. Department of Energy by Lawrence Livermore National Laboratory under Contract DE-AC52-07NA27344.

August 15, 2014

Plutonium Adsorption and Desorption from Bentonite: Progress Report FT-14LL0807071

James D. Begg[a], Mavrik Zavarin[a], Scott J. Tumey[b], Annie B. Kersting[a]

[a]Glenn T. Seaborg Institute, Physical & Life Sciences, Lawrence Livermore National Laboratory, 7000 East Avenue, Livermore, CA 94550, USA.
[b]Physical & Life Sciences, Lawrence Livermore National Laboratory, 7000 East Avenue, Livermore, CA 94550, USA.

Contents

1. Introduction

This progress report (FT-14LL0807071) summarizes research conducted at LLNL as part of the International collaborative effort within the UFD program. Burial in a deep geological repository is seen as the most viable option for radioactive waste disposal in many countries with a civilian nuclear fuel program.(Iaea, 1995) Conceptually, the repository scenario comprises a geological barrier (host rock) combined with engineering barriers that aim to contain the radionuclides until they have decayed below harmful levels. The waste itself will likely be contained in steel canisters surrounded by a layer of compacted clay. The efficacy of this disposal option is related to its capacity to confine radioactivity and isolate it from the biosphere.(Dozol et al., 1993)

Due to their swelling properties, plasticity, ion exchange and sorption behavior, and sealing capability, bentonites are good candidates for backfill material.(Guven, 1990) Traditionally, the term bentonite refers to aluminum phyllosilicate clays derived from the devitrification and chemical alteration of glassy volcanic ash or tuff.(Ross and Shannon, 1926) However, more recently the term has been used to describe smectite-rich materials, regardless of origin.(Grim, 1968) As a backfill material they are expected to both absorb stresses and deformations in the host rock and retard radionuclide migration. Radionuclide retardation is expected to be achieved by sorption processes that will render aqueous species immobile. Montmorillonites constitute a large proportion of bentonite mineralogy (65-90 wt %) with the result that the two names are often used synonymously, although the former is a clay mineral and the latter a clay rock.(Grauer, 1986) Montmorillonite clays are 2:1 dioctahedral smectites and can display significant morphological and chemical differences depending on their provenance.(Guven, 1988)

ENRESA, the body responsible for the management of Spanish radioactive waste, has identified a bentonite from Cortijo de Archidona in Almeria (Spain; FEBEX bentonite) for use in its repositories. As a result, the physiochemical properties of this clay have been well studied, particularly in an extensive experimental program performed at the National Cooperative for the Disposal of Radioactive Waste's (Nagra) Grimsel Test Site in Switzerland. The FEBEX clay has a high smectite content (93 ± 2 %) with quartz (2 ± 1%), plagioclase (3 ± 1 %), cristobalite (2 ± 1 %), potassium feldspar, calcite and trydimite as accessory minerals.(Missana et al., 2004) The structural formula for the less than 2 μm fraction (after Ca homoionization) is: $(Si_{7.78}Al_{0.22})(Al_{2.78}Fe^{3+}_{0.33}Fe^{2+}_{0.02}Ti_{0.02}Mg_{0.81})O_{20}(OH)_4(Ca_{0..50}Na_{0.08}K_{0.11})$.(Fernandez et al., 2004)

Due to their long half-lives and their abundance, the isotopes ^{239}Pu (2.41×10^4 y) and ^{240}Pu (6.56×10^3 y) are expected to contribute significantly to the total waste activity(Schwenk-Ferrero, 2013), meaning that plutonium may exert a significant biological threat in long term waste repository scenarios. Despite several decades of study, our understanding of how Pu migrates in subsurface environments is far from complete due to the wide array of factors which can significantly influence its mobility. These include Pu redox processes,(Choppin, 1991; Sanchez et al., 1985) colloid-facilitated transport processes,(Kersting et al., 1999; Novikov et al., 2006) solubility effects,(Efurd et al., 1998; Neck et al., 2007b) sorption/desorption rates and affinities for natural mineral surfaces(Powell et al., 2004; Zavarin et al., 2012), and interactions with natural organic matter (including bacteria)(Icopini et al., 2009; Zhao et al., 2011). Pu exhibits a complex redox chemistry in natural waters with four oxidation states (VI, V, IV, III) potentially stable and with each oxidation state displaying a unique solubility(Neck et al., 2007b) and mineral sorption affinity.(Begg et al., 2013; Keeney-Kennicutt and Morse, 1985; Sanchez et al., 1985; Silva and Nitsche, 1995) Pu(IV) and Pu(V) are the more common species under mildly oxic environmental conditions and also represent the oxidation states with the highest (Pu(V))

and lowest (Pu(IV)) predicted subsurface mobilities.(Choppin, 2007; Kaplan et al., 2007; Silva and Nitsche, 1995)

Colloid-facilitated transport is thought to be a significant contributor to Pu transport in the subsurface.(Kersting et al., 1999; Novikov et al., 2006; Santschi et al., 2002) One of the concerns with the use of bentonite as a backfill material in a repository is that it can form colloidal particles which may enhance the migration of radionuclide species which are sorbed to the bentonite.(Geckeis et al., 2004) As a result, attention has been focused on the interaction between Pu and bentonite colloids.(Huber et al., 2011; Missana et al., 2008) Previous work on FEBEX bentonite has shown that colloids with a hydrodynamic size of 250 ± 50 nm have an XRD pattern consistent with an aluminum-rich dioctahedral smectite with no significant impurities.(Missana et al., 2004)

The adsorption of Pu species to smectite minerals has been found to exhibit pH and ionic strength dependency, indicating that both ion-exchange and surface complexation processes are occurring.(Sabodina et al., 2006; Zavarin et al., 2012) However, surface complexation will dominate at neutral to alkaline pHs. Smectite minerals have been shown to have a high sorption affinity for Pu. For example, Pu(V) partitioning to Yucca Mountain tuffs found a ubiquitous and preferential association of Pu with smectite minerals.(Vaniman et al., 1995) Further, Pu(IV) K_d values from 10,000 to 40,000 mL g^{-1} have been reported for smectite-rich sediments in the pH range 5 to 12.(Lujaniene et al., 2007) Missana et al. (2008) studied the sorption of Pu(IV) onto FEBEX bentonite colloids at pH 9.5 and reported log K_d values of 5.37 ± 0.18 ml g^{-1}.(Missana et al., 2008) Pu(IV) sorption to FEBEX bentonite colloids under anaerobic conditions at pH 9.6, resulted in log R_d values (a term equivalent to K_d but without the assumption of equilibrium) of 5 and 5.9 after one and three weeks, respectively. The increase in R_d values with time was attributed to the presence of a small amount (~ 5 %) of Pu(VI) in the spike solution which was slowly reduced over time to Pu(IV) on the mineral surface.(Nagra, 2006) Recent work with SWy-1 montmorillonite and performed with both Pu(V) and Pu(IV) under aerobic conditions over a wide range of initial concentrations returned average log K_ds of 3.57 ±0.18 and 4.25 ± 0.15, respectively, after 30 days.(Begg et al., 2013) However, following one year of equilibration, calculated log K_d values in the Pu(V) experiments had increased to 4.32 ± 0.15. The convergence of K_d values for Pu(IV) and Pu(V) was attributed to the slow reduction of Pu(V) on the montmorillonite surface causing increased uptake of Pu(V). This finding highlights the need to ensure that experimental studies used to inform predictive transport models accurately encapsulate long term environmental behaviors.

One common problem of performing Pu(IV) adsorption experiments is its low solubility at circumneutral pH. In the presence of O_2, and the absence of complexing ligands, aqueous Pu(IV) concentrations are expected to be below 10^{-10} M depending on which Pu solid phase is most favorable.(Neck et al., 2007a) However, solubility studies have also shown that in solution, redox transformations will lead to Pu(V) species dominating Pu aqueous speciation, resulting in Pu concentrations greater than would be predicted for Pu(IV) alone.(Neck et al., 2007a; Neck et al., 2007b) One possible consequence of the low solubility of Pu(IV) is that sorption may demonstrate a concentration dependence as solubility limits are reached. For example, the study of Pu(IV) sorption to bentonite colloids observed that adsorption was linear for initial Pu concentrations of $1 \times 10^{-8} - 1 \times 10^{-7}$ M after which precipitation of Pu was observed.(Missana et al., 2008) Moreover, a study of Pu(IV) sorption to hematite found a difference in sorption kinetics with initial starting Pu(IV) concentrations of 10^{-14} M and 10^{-10} M which was attributed to formation of polymeric species at the higher concentration.(Romanchuk et al., 2011) Further, work with goethite and Np(V) found that K_d values differed by an order of magnitude at solution concentrations below 10^{-11} M compared to higher concentrations. This behavior was attributed to

the existence of different adsorption sites on the mineral with different adsorption affinities for Np.(Snow et al., 2013) These examples of concentration dependent behavior of actinides indicate that there may be a difference between the adsorption behavior of Pu at the concentrations found in contaminated subsurface waters (10^{-12} – 10^{-20} M)(Dai et al., 2005; Kersting et al., 1999; Novikov et al., 2006; Penrose et al., 1990) and concentrations typically used in laboratory experiments (ca. 10^{-10} M Pu). Although a primary assumption of reactive transport models, the validity of extrapolating Pu-montmorillonite sorption behavior from relatively high concentration laboratory experiments to the low concentrations found in many field settings has not been widely tested.

Pu desorption reactions have been far less well studied than adsorption reactions. This is problematic because application of thermodynamic equilibrium parameters in field transport models which incorrectly represent desorption processes are likely to be flawed.(Artinger et al., 2002) One of the pertinent issues for Pu, especially given the evidence that its mobility may be enhanced by colloid facilitated transport, is whether there is equality in adsorption and desorption behavior.(Kersting et al., 1999) Differences in behavior may be caused by aging processes, hysteresis effects, and irreversible sorption, amongst others.(Tinnacher et al., 2011) A study of Pu(IV) sorption to Callovo-Oxfordian argillite found that after seven days' desorption, Pu K_d values were of the same order of magnitude as they were following a seventy four day adsorption period indicating sorption reversibility.(Latrille et al., 2006) Similarly, Lu et al investigated Pu interaction with montmorillonite and found that with a 20 day adsorption period and a 32 day desorption period, similar K_d values were obtained for both adsorption and desorption steps.(Lu et al., 2003) However, while these experiments suggest that Pu displays sorption reversibility for clays, they do not provide information on the kinetics of desorption which are important for predicting colloid facilitated transport.

Previously we investigated the adsorption of Pu(V) to SWy-1 montmorillonite at initial concentrations of 10^{-6} to 10^{-16} M.(Begg et al., 2013) The isotherm obtained after 30 days of adsorption was broadly linear for this wide range of Pu(V) concentrations. The aim of the current work is two-fold: to provide information on Pu adsorption/desorption to FEBEX bentonite, a potential repository backfill material, and to determine if the linearity observed for Pu(V) sorption to a pure clay mineral extends is replicated for Pu(IV) sorption to a multi-component clay rock. We investigate the sorption behavior of Pu(IV) to FEBEX bentonite across a wide range of initial concentrations (10^{-7} – 10^{-16} M) over a 120 d period. In addition, we perform long term (10 month) adsorption experiments with Pu(V) to better constrain the slow apparent rates of reduction on bentonite. These results of these experiments demonstrate the control that the montmorillonite in bentonite exerts on the adsorption behavior of Pu, provides long term adsorption data for Grimsel test site experiments, and validates the extrapolation of Pu(IV) experiments performed at concentrations of 10^{-10} M Pu to concentrations typically found in the environment at timescales relevant for groundwater transport.

2. Materials and Methods

2.1 Bentonite Preparation

Unless stated otherwise, all solutions were prepared using ultrapure water (Milli-Q Gradient System, >18 MΩ·cm) and ACS grade chemicals without further purification. The FEBEX bentonite was ground in a mortar and pestle and sieved to <63 μm. The clay was then homo-ionized in 1 M NaCl solution for 7 days and dialyzed in MQ H_2O to remove excess salts. As

experiments were performed to characterize the behavior of Pu in the presence of bulk bentonite, no further treatment was performed. A portion of the bentonite suspension was dried, the clay lightly ground and its surface area measured (N_2(g)-BET Quadrasorb SI). The surface area of the prepared bentonite was 25.2 ± 1.0 m^2 g^{-1}.

The solids were re-suspended in a 0.7 mM $NaHCO_3$, 5 mM NaCl buffer solution (pH 8) to make a suspension with a bentonite concentration of ~ 5 g kg^{-1}. Gravimetric analysis of the mass of solid in triplicate 5 mL aliquots of the suspension returned a standard error of 1.2% indicating homogeneity in the stock suspension and providing confidence in the amount of solid added to experiments. The stock suspension was allowed to equilibrate for several days prior to the start of sorption experiments.

2.2 Pu Stock Solutions

Three different Pu stock solutions were used in the adsorption experiments in order to facilitate measurement of the wide range of Pu concentrations used. A ^{242}Pu stock (15.8% ^{238}Pu, 5.1% $^{239+240}$Pu, 79.1% ^{242}Pu by activity) and a ^{238}Pu stock (98.8% ^{238}Pu, 0.11% ^{241}Pu, and 0.1% ^{239}Pu by activity) were used in experiments with initial concentrations of 10^{-7} – 10^{-11} M. A New Brunswick Laboratory (NBL) Pu reference material CRM-137 (33.5% ^{238}Pu, 35.3% ^{239}Pu, 31.3% ^{240}Pu by activity) was used in experiments with initial Pu concentrations ≤ 10^{-11} M.

The Pu stock solutions were purified using anion exchange resin (BioRad AG 1 × 8, 100-200 mesh) pre-conditioned with 8 M HNO_3. Prior to loading on the resin, Pu was reacted with $NaNO_2$ to reduce it to Pu(IV). The Pu was loaded on the resin in 8 M HNO_3, washed with 3 column volumes of 8 M HNO_3, and then eluted in 0.1 M HCl.(Powell et al., 2011) For experiments using Pu(IV), the oxidation state of the Pu stocks was checked with a LaF_3 precipitation method (Kobashi and Choppin, 1988) and found to be > 97 % Pu(III)/(IV). Subsequent stock dilutions were made using 0.1 M HCl with select analysis indicating that this did not significantly alter the oxidation state of the Pu. For experiments starting with Pu(V), the Pu(IV) stripped from the columns was converted to Pu(VI) either electrochemically (^{242}Pu stocks) or by heating in HNO_3 (^{238}Pu stocks), adjusted to pH 3 with NaOH, spiked with 0.05 M hydrogen peroxide and gently heated to produce Pu(V). To remove any Pu(VI) remaining in solution, the stocks were diluted in 0.7 mM $NaHCO_3$, 5 mM NaCl buffer solution to achieve a circumneutral pH and contacted with 10 g/L high surface area SiO_2 which will preferentially adsorb Pu(VI).(Orlandini et al., 1986) Pu(V) stocks were less than 3% Pu(IV) by La F_3 precipitation. Final Pu concentration in the stock solutions was determined by LSC (Packard Tri-Carb TR2900 LSA and Ultima Gold cocktail).

2.3 Plutonium Batch Sorption Experiments

Sorption experiments were performed over a wide range of initial Pu(IV) concentrations (10^{-7} – 10^{-16} M). In the following description we use the nominal terms *high concentration* to refer to experiments initially spiked to Pu concentrations of 10^{-7} – 10^{-11} M and *low concentration* for experiments initially spiked to Pu concentrations of 10^{-11} – 10^{-16} M. The two types of experiments were performed in separate laboratories in order to minimize any potential contamination of the *low concentration* samples.

All Pu(IV) and Pu(V) batch sorption experiments were performed under air in 0.7 mM $NaHCO_3$, 5 mM NaCl buffer solution (pH 8) with 1 g L^{-1} bentonite. Pu(IV) and Pu(V) aqueous speciation

for initial Pu concentrations of 10^{-10} M in the buffer solution were calculated using the Geochemist's Workbench family of codes and thermodynamic data from Guillaumont et al. (2003).(Guillaumont et al., 2003) The results are shown in Figure 1. Batch experiments were conducted in either 50 mL Nalgene Oak Ridge polycarbonate centrifuge tubes (*high concentration*) or 500 mL Nalgene bottles (*low concentration*). Higher volumes were required in *low concentration* experiments to achieve the low detection limits afforded by AMS. Pu(IV) sorption experiments were performed at *low concentrations* and *high concentrations*, while Pu(V) experiments were performed only at *high concentrations*. For Pu(IV) experiments, where the stock solution was in 0.1 M HCl, NaOH was added to the samples immediately prior to spiking in order to neutralize the acidity associated with the Pu(IV) spike. This was not necessary for Pu(V) experiments where the pH of the stock solution was circumneutral. Bentonite blanks (with no Pu) and Pu spiked blanks (with no bentonite; select concentrations) were run in parallel. The pH of each experiment was checked (Orion 920A with calibrated electrode) and adjusted to pH 8.0 ± 0.2 using dilute NaOH or HCl within 10 minutes of spiking. Measurement of pH over the course of the experiments indicated that the drift in pH was less than 0.2 pH units. Samples were placed on an orbital shaker at 125 rpm at room temperature for the duration of the experiment. Experiments were kept in the dark in order to minimize photo-catalyzed reactions that may directly or indirectly affect the redox speciation of Pu.(Mccubbin and Leonard, 1996; Powell et al., 2005)

At each time point, samples were centrifuged to achieve a 50 nm size cut off. In *high concentration* experiments, both aliquots of the suspension and the supernatant were removed and counted via LSC. In *low concentration* experiments, aliquots of supernatant were acidified to 2% HNO_3 and analyzed using AMS (10-MeV tandem accelerator at the Center for Accelerator Mass Spectrometry (CAMS), Lawrence Livermore National Laboratory, CA. AMS is an ultra-sensitive analytical technique that can quantify long-lived radionuclides at ultra-low concentrations and routinely achieves instrumental backgrounds of 10^5 atoms for actinide elements. (Marchetti et al., 2005)AMS analysis has been reported previously and included isotope dilution using a non-isobarically interfering isotope of ^{242}Pu (99.99% ^{242}Pu).(Marchetti et al., 2005)

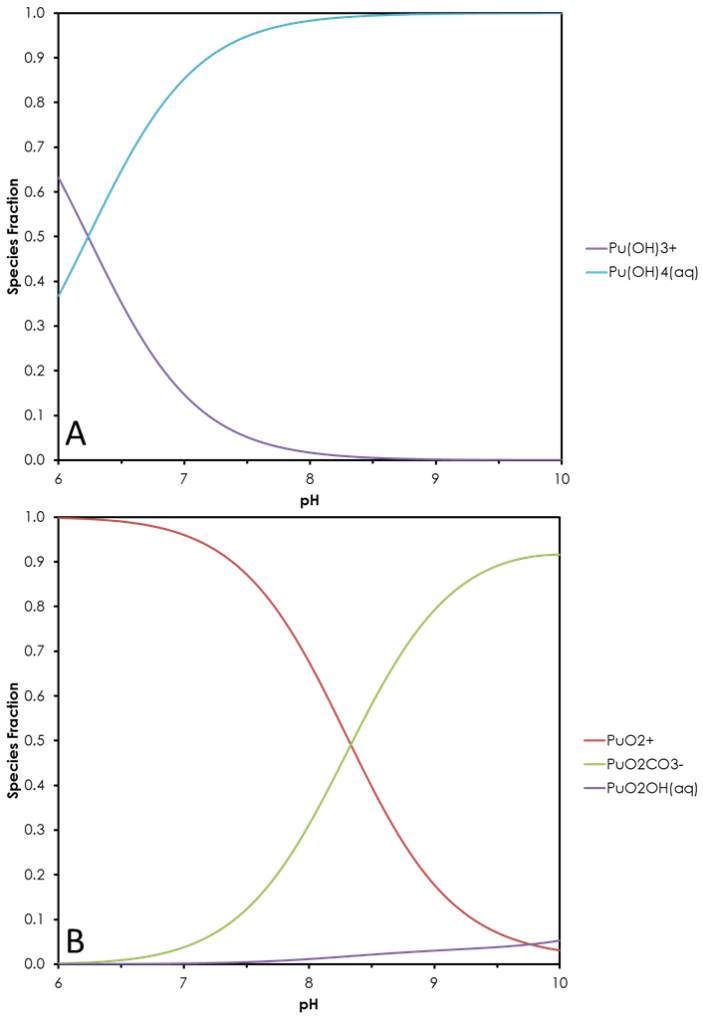

Figure 1. Predicted speciation of Pu(IV) (A) and Pu(V) (B) in experimental systems used in this study ([Pu] 10^{-10} M; 0.7 mM $NaHCO_3$, 5 mM NaCl buffer solution at pH 8). Calculations performed using thermodynamic constants from Guillaumont et al. (2003).(Guillaumont et al., 2003) Other species which were accounted for but were not significant over this pH range were $Pu(CO_3)^{4-}$, $Pu(CO_3)_5^{6-}$, $Pu(OH)^{2+}$, $Pu(OH)_3^{+}$, Pu^{4+}, $PuCl^{3+}$ and $PuOH^{3+}$ for Pu(IV) and $PuO_2(CO_3)_3^{5-}$ for Pu(V).

2.4 Plutonium Desorption Flow Cell Experiments

A stirred flow cell experiment was performed at pH 8 to examine the desorption of Pu(IV) from bentonite. The flow cell set up was similar to that described previously for Np(V) reaction with goethite.(Tinnacher et al., 2011) The flow cell was made of Teflon®, with a 20 mL hemispherical chamber and fitted with a 100 nm pore size Millipore polycarbonate filter. A diagram of the flow cell is shown in Figure 2. Prior to use, the cell was washed with 10% HCl and MQ water. To adsorb Pu on the clay, Pu(IV) at 3×10^{-10} M was equilibrated with 1 g L^{-1} bentonite for 21 days to be consistent with previous flow cell experiments performed in our lab.(Begg et al., 2014) After this equilibration period, an aliquot of the spiked suspension was centrifuged (25 000 × g, 2 h; 50 nm cut-off) and the concentration of the Pu in the supernatant measured. A 20 mL aliquot of

bentonite suspension was loaded into the flow cell with a stir bar included to ensure ideal mixing conditions. In previous flow cell work with montmorillonite, ^{3}H was used as a conservative tracer to test if ideal mixing conditions existed in the cell. A plot of the decline in ^{3}H concentration and a theoretical non-reactive species is shown in Figure 3. The similarity between the calculated and observed curves demonstrates that the flow cell experiment is ideally mixed.

Atmosphere-equilibrated, Pu free 0.7 mM $NaHCO_3$, 5 mM NaCl buffer solution at pH 8 was flowed through the cell at an initial rate of 0.4 mL min^{-1} (average retention time of ~ 50 minutes). Effluent fractions were collected on a Spectra/Chrom CF-1 fraction collector and the volumes determined gravimetrically. Periodic pH measurements of the effluent were performed to ensure that the experiment remained at pH 8. Collected fractions were acidified with 2% HNO_3 prior to Pu analysis. Pu concentration in the effluent fractions was determined via liquid scintillation counting.

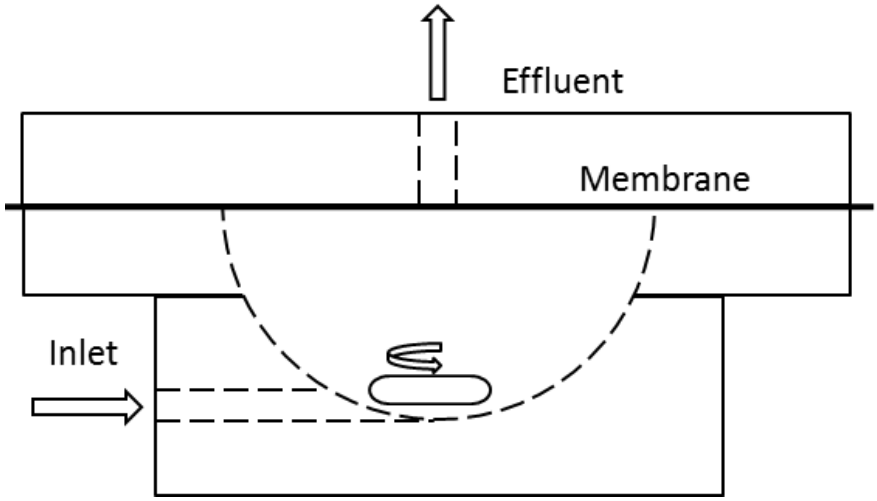

Figure 2. Flow cell set up. Cell provided by Dr Brian Powell (Environmental Engineering and Earth Sciences, Clemson University). Figure provided by Jennifer Wong (Environmental Engineering and Earth Sciences, Clemson University).

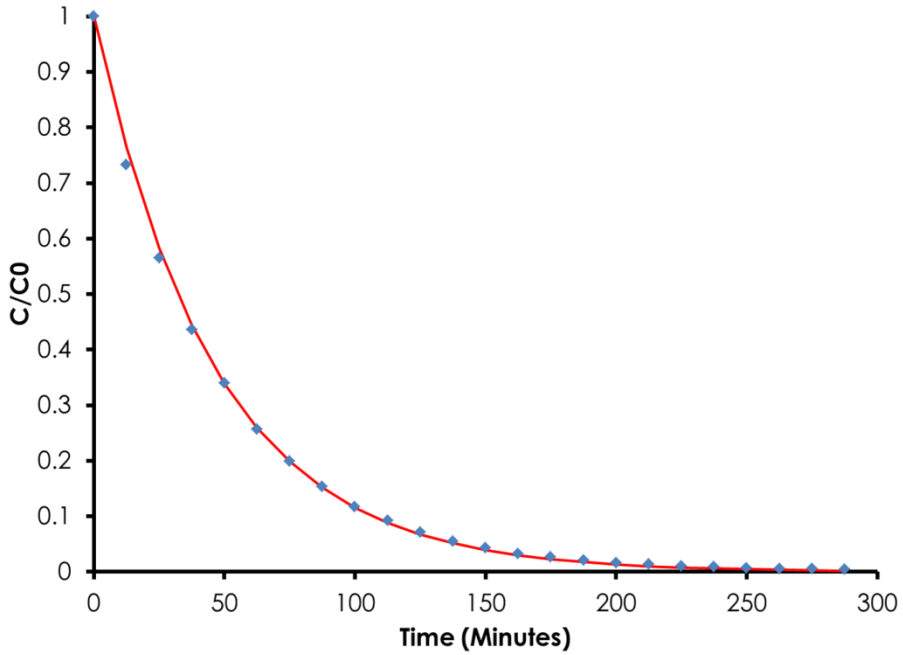

Figure 3. ^{3}H effluent profile from flow-cell experiment performed with montmorillonite. Data points represent measured fraction of ^{3}H in effluent. Solid line represents theoretical non-reactive tracer . Flow rate = 0.4 mL min^{-1}, cell volume = 20 mL.

In order to evaluate the kinetic nature of desorption, the flow rate was changed after approximately 10 chamber volumes (cv) had been passed through the cell to 0.2 mL min^{-1} (100 minute residence time). After a further 10 cv the flow rate was changed to 0.04 mL min^{-1} (500 minute residence time) and again after a further 10 cv to 0.02 mL min^{-1} (1000 minute residence time). The total timescale of the flow cell experiment was 12 days.

3. Results and Discussion

3.1 Pu(IV) Adsorption to Bentonite

The sorption of Pu(IV) to bentonite was studied over an initial Pu concentration range of 10^{-7} – 10^{-16} M. The resulting adsorption isotherm after 120 d equilibration is shown in Figure 4. To determine if adsorption equilibrium was achieved in the experiment, samples at 10^{-10} and 10^{-8} were sampled after 67 d, 100 d and 120 d. The results of this sampling are shown in the inset in Figure 4. The similarity in the aqueous Pu concentrations at 100 d and 120 d versus 67 d indicate that adsorption equilibrium was reached by 120 d. The slow approach to sorption equilibrium is consistent with previous studies on Pu(IV) sorption to clay and may reflect the presence of small amounts of Pu(V) in the initial stock solution.(Begg et al., 2013; Nagra, 2006) Alternatively, unintended changes in Pu oxidation state may be exacerbated when an acidic Pu(IV) stock is spiked into a circumneutral pH solution under oxic conditions. Figure 5 shows oxidation state analysis of a pH 8 solution spiked with a >97% Pu(III)/(IV) stock solution. Both LaF_3 and solvent extraction analysis of the aqueous Pu indicate that 1 h after spiking, approximately 30% of the Pu(III)/(IV) had been oxidized. LaF_3 analysis over 6 d showed no appreciable change in Pu oxidation state from the 1 h values.

After 120 days of equilibration, the sorption of Pu(IV) to bentonite clay was broadly linear over the ten orders of magnitude concentration range tested (Figure 4). This result complements the linear sorption behavior observed for Pu(V) on montmorillonite over a similar Pu concentration range.(Begg et al., 2013) This result shows that at the macroscale and on timescales on the order of months, Pu(IV) exhibits similar adsorption behavior to smectite clay at the higher concentrations used in typical laboratory experiments (10^{-8} – 10^{-10} M) as it does at concentrations typically found in contaminated environments (< 10^{-12} M). This result was previously seen for Pu(V) sorption to smectite clay.(Begg et al., 2013)

Previous work with Pu(IV) and hematite identified a concentration dependence to the rate of Pu(IV) sorption.(Romanchuk et al., 2011) A one-step, fast adsorption was seen in experiments with 10^{-14} M Pu compared to a two-step adsorption (fast initial sorption followed by slower uptake) at 10^{-10} M Pu. The fast sorption step was attributed to the adsorption of monomeric Pu(IV) while the slower uptake was explained by either slow diffusion to micropores in the mineral or the formation of polymeric Pu(IV) species.(Romanchuk et al., 2011) However, the current work indicates that regardless of initial sorption rates, the extent of Pu(IV) sorption on bentonite is independent of initial concentration for the 10^{-7} – 10^{-16} M range on timescales of relevance to groundwater transport scenarios.

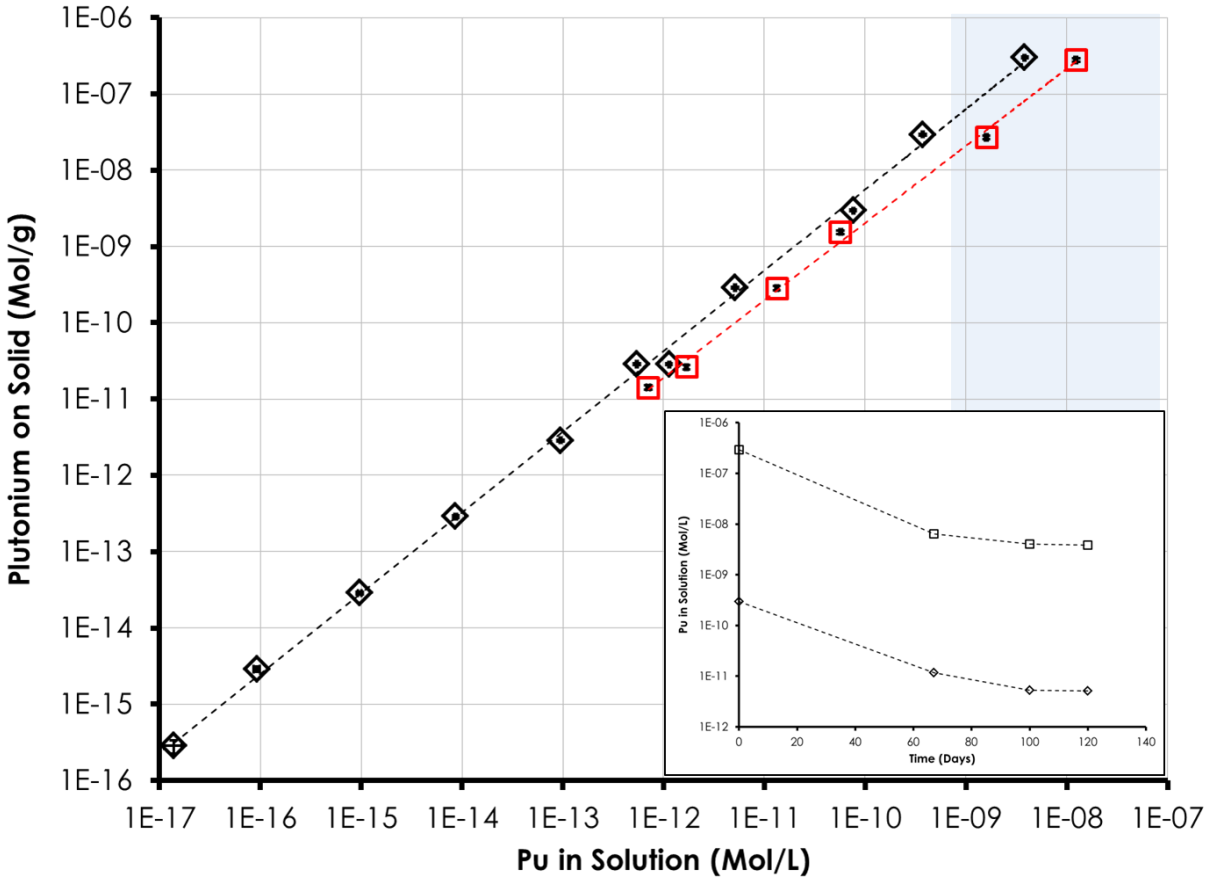

Figure 4. 120 d Pu(IV) sorption isotherm for FEBEX bentonite (1 g L^{-1}) in 0.7 mM $NaHCO_3$, 5 mM NaCl buffer solution at pH 8 (diamonds). Inset shows time series data for experiments at 10^{-7} and 10^{-10} M initial

Pu(IV) to indicate apparent adsorption equilibrium at 120 d. Also shown are data for 30 d Pu(IV) adsorption isotherm for SWy-1 Na-montmorillonite (1 g L^{-1}) in 0.7 mM $NaHCO_3$, 5 mM NaCl buffer solution at pH 8 (squares).(Begg et al., 2013) Lines are shown to guide the eye only. Error bars propagated from counting uncertainties for bentonite experiments and extrapolated from the standard deviation at the 1σ level for a representative experiment performed in quadruplicate for montmorillonite experiments.

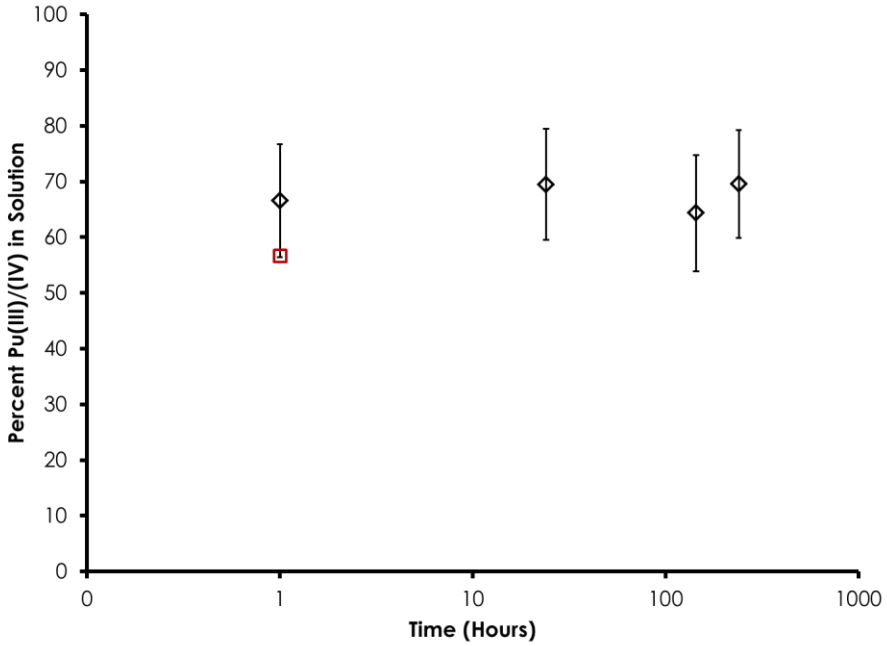

Figure 5. Percent Pu(III)/(IV) of solution Pu in 0.7 mM $NaHCO_3$, 5 mM NaCl buffer (pH 8) as measured by LaF_3 precipitation (diamonds). Also shown is percent Pu(IV) in solution as measured by solvent extraction at 1 h (square). Original Pu(IV) stock solution was > 97% Pu(III)/(IV) (LaF_3). Error bars are an estimated absolute 10% value and are intended to reflect the difference between the solvent extraction and LaF_3 precipitation techniques.

Also shown in Figure 4 is the 30 d adsorption isotherm for Pu(IV) on montmorillonite previously reported in Begg et al (2013).(Begg et al., 2013) Comparison of the Pu(IV) sorption isotherms for montmorillonite and bentonite shows they are quite similar in terms of slope and the extent of Pu sorption. These results indicate that Pu adsorption by bentonite (92% montmorillonite) is comparable to the adsorption to pure montmorillonite and that the other minor mineral phases are unlikely to be contributing significantly to the overall Pu adsorption behavior. However, a slightly higher adsorption affinity of Pu(IV) for bentonite than montmorillonite is observed and is more marked at the two highest Pu concentrations. Given that the current work suggests that adsorption equilibrium is not achieved after 67 d (Figure 4 inset), we suggest that this difference is in part due to the different equilibration period in the two experiments: 30 days for montmorillonite and 120 days for bentonite.

The expected concentration range for Pu(IV) colloid formation at pH 8 is also highlighted in Figure 4.(Neck et al., 2007b) The highest concentrations used in these isotherm experiments fall within the expected range for Pu(IV) colloid formation.(Neck et al., 2007b) This may mean that Pu(IV) colloid formation also contributes to the adsorption behavior of Pu in these experiments.

For example, the log-log slope for Pu(IV) sorption to bentonite is 1.05 ± 0.01 when all the data points are considered. A value greater than 1 indicates a process other than monomeric adsorption is occurring on the surface of the bentonite.
As the isotherm slope is close to unity, sorption can be considered Langmuirian in behavior. However, unlike traditional Langmuir plots which exhibit a flattening of the isotherm as mineral surface sites become saturated, the data remain linear at higher concentrations. Previously, Missana et al. (2007) calculated the strong site concentration on bentonite colloids to be 6.1×10^{-8} mol m^{-2}.(Missana and Garcia-Gutierrez, 2007) Given the that experiments were performed with 1 g L^{-1} clay with a surface area of 25 m^2 g^{-1} this would provide a total strong site concentration of 1.54×10^{-6} mol L^{-1} in the current experiments which is greater than the highest Pu concentration used (10^{-7} M). As a result, strong site saturation effects are not expected in these data.

Mineral free experiments were performed with initial Pu(IV) concentrations of 10^{-8}, 10^{-9} and 10^{-11} M Pu(IV). Measurement of the aqueous phase (i.e. with no centrifuging) within 1 d of spiking and again after 120 d showed that 60-75 % of Pu was lost from the bulk solution over the course of these experiments. These results indicate that either precipitation of Pu(IV) colloids followed by sorption to container walls or sorption of monomeric Pu(IV) to container walls will occur in the absence of a mineral surface under the experimental conditions. However, in *high concentration* experiments performed with bentonite, both bulk suspension and aqueous Pu concentrations were analyzed with LSC. Measurement of these two phases indicated that the Pu(IV) was preferentially associated with the mineral phase rather than the container walls. Interestingly, LaF_3 analysis of the 10^{-10} M Pu(IV) mineral free experiment performed after 120 d indicated that the dominant oxidation state in the solution was Pu(V)/(VI).

Log K_d values for the Pu(IV) bentonite sorption isotherm range from 4.3 – 4.9 mL/g compared to values of 3.9 - 4.4 ml/g observed for Pu(IV) sorption to montmorillonite colloids.(Begg et al., 2013) There was a slight increase in calculated log Kd values as a function of Pu(IV) concentration. We attribute this to Pu(IV) colloid formation and/or other precipitation processes at the higher concentrations, as discussed previously, rather than the result of concentration-dependent, high sorption affinity sites on the clay which would exibit an inverse relationship between Kd and Pu(IV) concentration. The K_d values observed in this experiment are lower than the values observed for Pu(IV) sorption to bentonite colloids of 5-5.9 mL g^{-1} measured by Geckeis et al.(Geckeis et al., 2004) and 5.39 ± 0.18 measured by Missana et al.(Missana et al., 2008) However, these previous experiments were performed at pH 9.5 – 9.6 and used bentonite colloids of ~200 - 280 nm. Which are expected to be entirely composed of montmorillonite.(Huber et al., 2011) Thus, our results indicate that although sorption to the < 63 μm size-fraction and the colloid size-fraction is largely similar, there is sufficient difference in behavior to warrant caution when informing reactive transport models.

3.2 Pu(V) Adsorption to Bentonite

The adsorption of Pu(V) to bentonite was studied over a 30 day period using an initial concentration of 10^{-10} M (Figure 5). Also plotted in Figure 5 is the adsorption of Pu(V) to montmorillonite at an initial concentration of 10^{-9} M reported previously.(Begg et al., 2013) Both adsorption plots show a similar profile, suggesting that, as with Pu(IV) sorption, the montmorillonite component of bentonite is responsible for the adsorption of Pu(V). The adsorption of Pu(V) by bentonite shows an initial rapid uptake with 49.5% ± 0.7 % removed in the first 48 h. This is followed by a slower uptake over the rest of the 30 d experiment with 13.4 ± 1.6 % Pu remaining in solution at this time. Applying the first order rate model previously used to

describe Pu(V) adsorption to montmorillonite to the bentonite-Pu(V) adsorption data leads to a surface area normalized adsorption rate of $10^{-3.5}$ L m^{-2} h^{-1} which compares favorably with $10^{-2.8}$ L m^{-2} h^{-1} previously reported for Pu(V) adsorption to montmorillonite.(Begg et al., 2013)

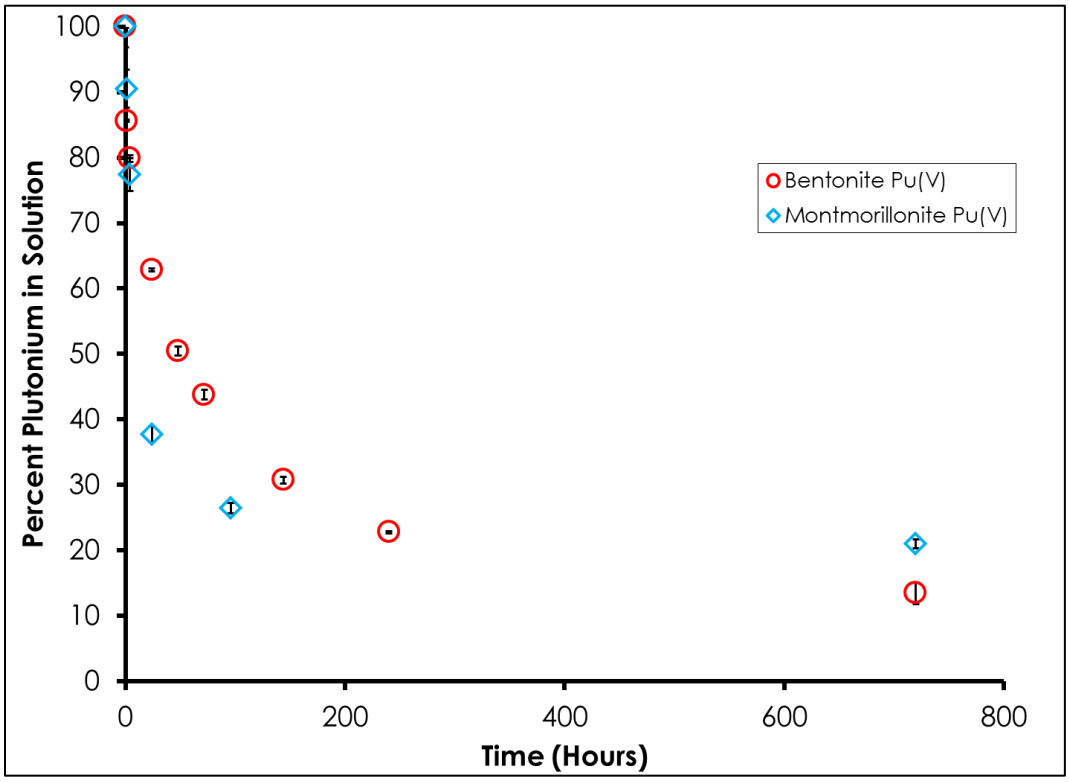

Figure 5. Sorption of Pu(V) to FEBEX bentonite (1 g L^{-1}; circles) and SWy-1 Na-montmorillonite (1 g L^{-1}; diamonds) plotted as percentage of Pu removed from solution vs time. Initial Pu concentrations were 10^{-10} M for bentonite and 10^{-9} M for montmorillonite. Error bars represent the standard deviation at the 1σ level for triplicate bentonite experiments and are propagated from the standard deviation at the 1σ level for representative quadruplicate montmorillonite experiments.

The adsorption of Pu(V) to bentonite was studied over an initial concentration range of 10^{-7} – 10^{-11} M Pu. Samples were analyzed after 30, 120 and 300 d. At 30 days, the isotherm is linear on a log-log plot with slope of 0.92 ± 0.03 (Figure 6). However, the slope of 0.92 indicates that sorption is, in fact, non-linear and appears to exibit a Freundlich behavior (i.e. $S=K_fC^n$ with n=0.92). At 120 d, the isotherm is truly linear with a log-log slope of 1.03 ± 0.03. As was observed in Pu(V) experiments with montmorillonite sampled at 30 d and 1 year, the position of the isotherm has shifted, indicating that adsorption of Pu from the aqueous phase has continued over the time period between 30 and 120 d. At 300 d, the isotherm was again linear (1.02 ± 0.001), with a further small shift in position relative to the 120 d isotherm.

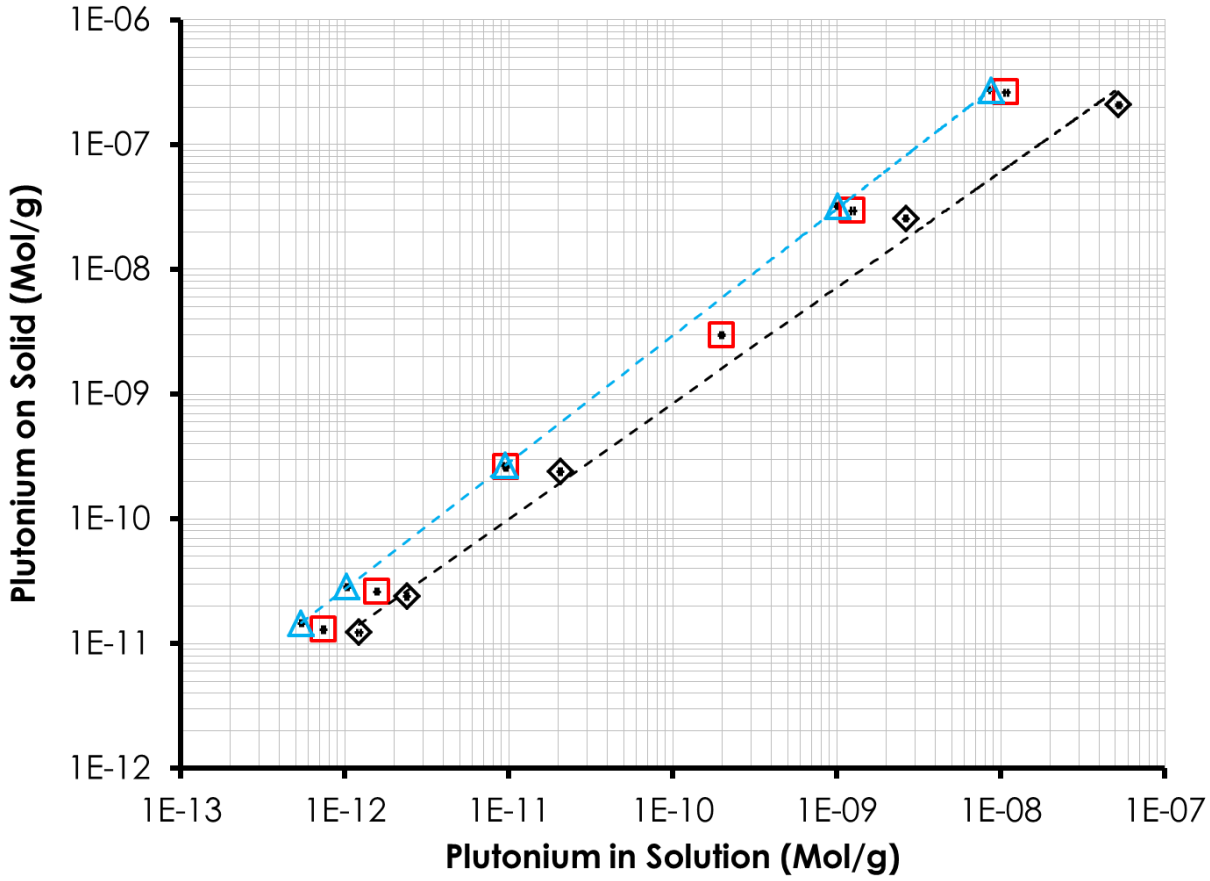

Figure 6. Pu(V) sorption isotherm to FEBEX (1 g L^{-1}) in 0.7 mM $NaHCO_3$, 5 mM NaCl buffer solution at pH 8. Different symbols represent sampling at different time points: 30 d (diamonds), 120 d (squares), 300 d (triangles). Lines are to guide the eye only. Error bars propagated from counting uncertainties for bentonite experiments.

The Pu(V) adsorption data for 30 d and 300 d is plotted alongside the 120 d Pu(IV) adsorption data in Figure 7. Over the course of the experiment, the position of the Pu(V) adsorption data moves towards the 120 d Pu(IV) adsorption data. This observation is consistent with the idea that kinetically limited reduction of Pu(V) on the mineral surface is responsible for the slow, continued uptake of Pu. Log K_d values for Pu(V) sorption to bentonite after 300 days were 4.42±0.03. The similarity of the K_d values of both Pu(IV) and Pu(V) over these long timescales demonstrates a convergence of the adsorption behavior of Pu regardless of initial oxidation state.

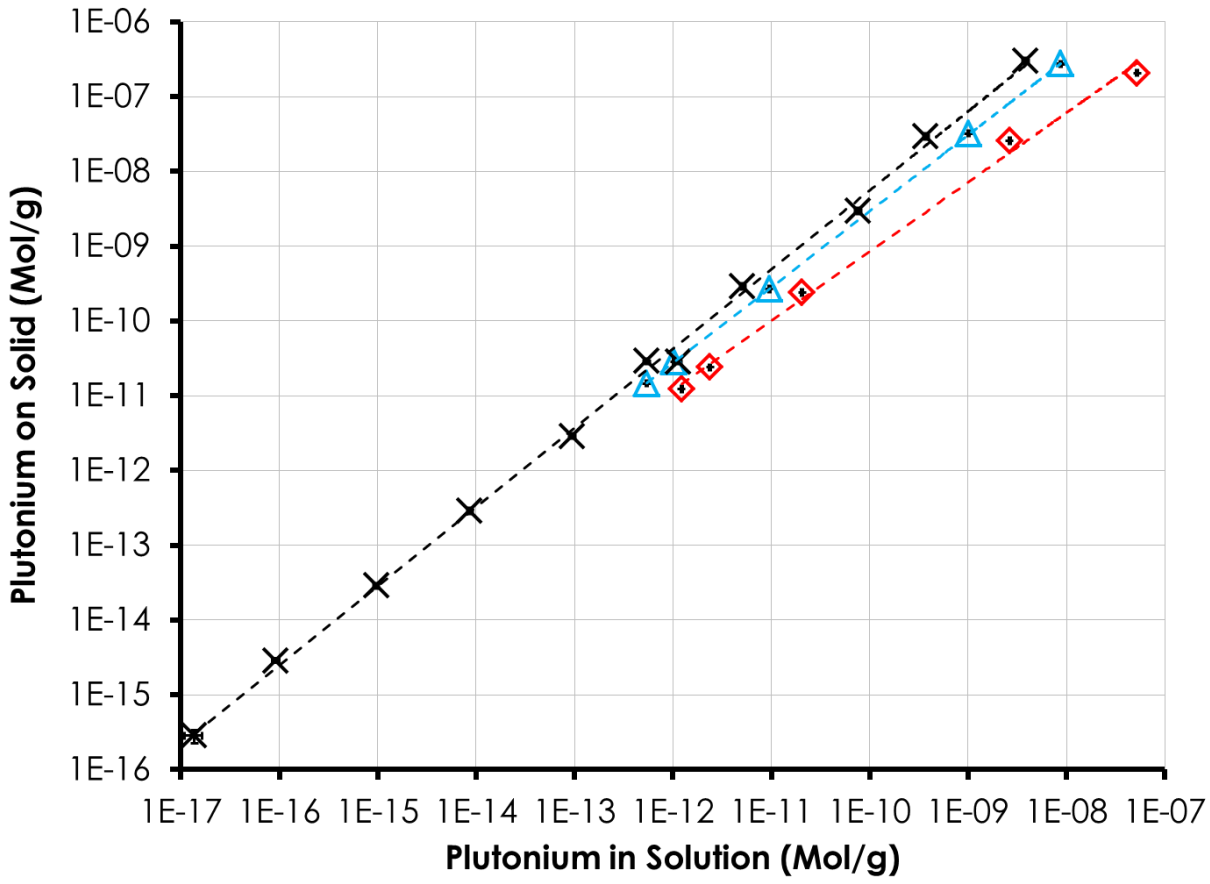

Figure 7. Sorption of Pu(V) to FEBEX bentonite (1 g L^{-1}, pH 8) at 30 d (diamonds) and 300 d (triangles), shown with Pu(IV) sorption to FEBEX bentonite (1 g L^{-1}, pH 8) at 120 d (crosses). Error bars propagated from counting uncertainties for bentonite experiments

By assuming that the slow uptake of Pu from solution seen in the Pu(V) isotherm was due to the slow reduction of Pu(V) on the clay surface, the data from the 30 d, 120 d, and 300 d time points was used to constrain the apparent reduction rate. By using these last three data points, we hope to remove better isolate the reduction process from the early time adsorption of Pu(V).(Begg et al., 2013) Apparent first order reduction rates were calculated from the slope of the plot of ln(C) versus time. The log average surface normalized apparent reduction rate for these experiments was $10^{-5.3\pm1.3}$ L m^{-2} h^{-1}. Interestingly, when the same calculation was applied to the Pu(IV) data collected at 10^{-10} M for 67, 100 and 120 d, the calculated rate was $10^{-4.6\pm0.7}$. The similarity between the values further suggests that the long term uptake observed in Pu(IV) experiments is likely due to reduction of residual Pu(V).

Mineral free Pu(V) experiments were performed at initial concentrations of 10^{-10} and 10^{-8} M. A loss of Pu from solution was observed in both experiments with 73% and 36% remaining in solution in the 10^{-10} M an 10^{-8} M Pu(V) experiments, respectively, after 300 d. It is possible that adsorption to the container walls is responsible for this loss of Pu from solution. However, the difference in loss between the two concentrations also indicates that Pu precipitation may play a role in the removal of Pu from solution. This is consistent with previous work that has shown the solubility of Pu(V) in natural waters at circumneutral pH to be in the range of 10^{-6} – 10^{-9} M.

Further, previous work in our lab has observed differences in the behavior of aqueous Pu(V) in mineral free experiments at concentrations of 10^{-6} and 10^{-9} M.(Begg et al., 2013; Neck et al., 2007b; Nitsche and Edelstein, 1985; Runde et al., 2002)

The oxidation state of Pu in solution was monitored for bentonite experiments performed at 10^{-10} M and 10^{-8} M Pu(V) using LaF_3 precipitation (Figure 8). In both experiments, the percentage of Pu(V)/(VI) as a total of Pu in solution declines between 30 and 120 days. At 300 d, the percent Pu(V)/(VI) in solution was 33±11% and 33±26% in experiments at 10^{-10} M and 10^{-8} M, respectively. In contrast, in mineral free Pu(V) experiments, LaF_3 analysis showed that the Pu remaining in solution after 300 days was dominated by Pu(V)/(VI) (96±10% and 75±18% for experiments at 10^{-10} and 10^{-8} M, respectively). This difference in oxidation state behavior between bentonite and mineral free experiments indicates that interaction of Pu with mineral surfaces results not only in surface mediated reduction of Pu(V) but also leads to a difference in oxidation state distribution in solution compared to Pu in solution when no mineral phase is present.

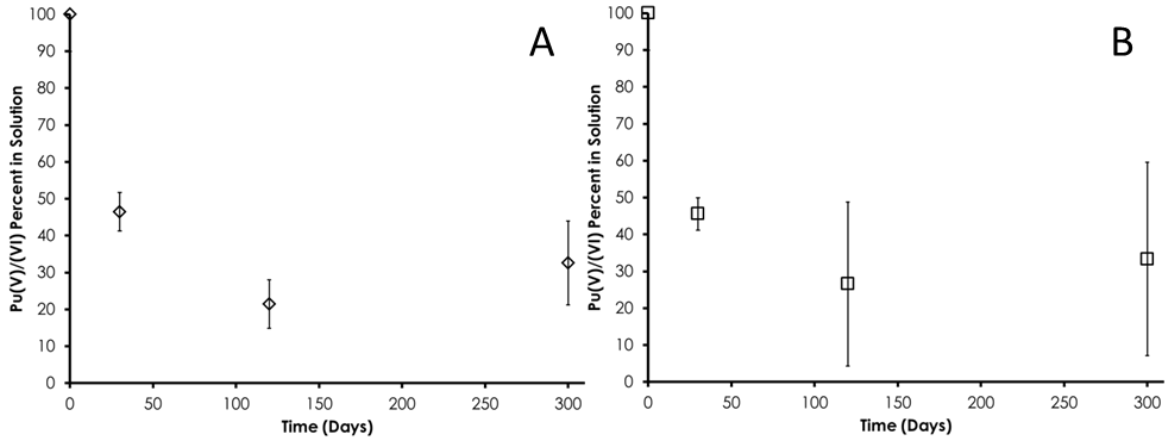

Figure 8. Changes in percent Pu(V)/(VI) in solution for Pu(V) isotherm experiments performed at initial concentrations of 10^{-10} M (A) and 10^{-8}M (B). Error bars based on propagation of LSC uncertainties

3.3 Desorption of Pu from Bentonite

A flow cell experiment was performed to investigate the desorption of Pu from bentonite. Prior to the desorption, Pu(IV) at an initial concentration of 3×10^{-10} M was equilibrated with 1 g L^{-1} bentonite in 0.7 mM $NaHCO_3$, 5 mM NaCl buffer solution at pH 8 for 21 days. After this period, the calculated log Kd for Pu sorption was 4.1 which is consistent with the long term adsorption behavior of the Pu(IV) isotherm experiment performed at 10^{-10} M (4.4 at 67 d, 4.8 at 120 d).

The desorption of Pu from bentonite is plotted as a fraction of total Pu in the system in Figure 9. The initial decline in the desorbed Pu fraction and large rise observed after 2 chamber volumes is an artifact of a stir bar malfunction between 0 and 2 cv which led to non-ideal mixing conditions in the flow cell. Between 0 and 5 cv, most (but not all) of the Pu in the effluent, represents aqueous Pu remaining in solution following the adsorption period. This Pu is displaced from the flow cell over the course of several cv (i.e. tailing). Ignoring the period between 0 and 2 cv, comparison of a theoretical non-reactive tracer dilution curve under the initial flow conditions

with the observed Pu concentrations shows that the two curves begin to deviate within 60 minutes (1.2 chamber volumes; Figure 10). The deviation demonstrates an excess of Pu in the effluent from that which would be expected by dilution alone, indicating that Pu desorption from bentonite contributes significantly to the overall Pu breakthrough after just a few pore volumes.

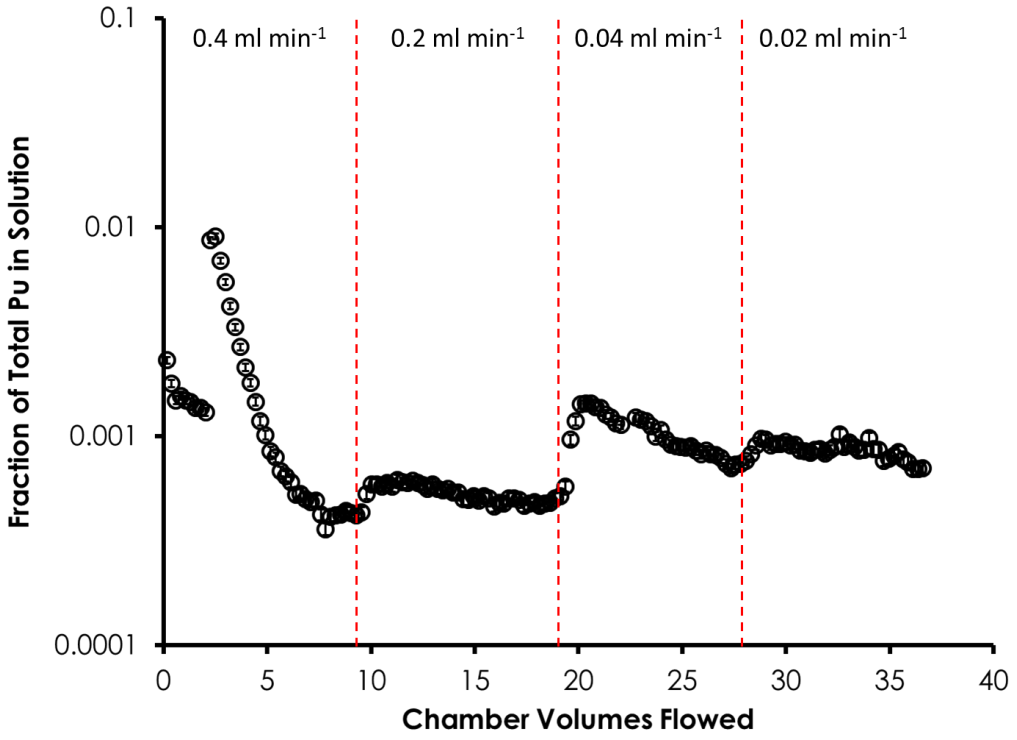

Figure 9. Pu aqueous concentration in the flow-cell effluent expressed as a fraction of total Pu concentration in the flow cell. System parameters: Cell volume = 20 mL; Background solution: 5 mM NaCl, 0.7 mM $NaHCO_3$, pH 8; Solid: solution ratio 1 g L^{-1}. Flow rates and residence times: (A) 0.4 mL min^{-1}, 50 minutes; (B) 0.2 mL min^{-1}, 100 minutes; (C) 0.04 mL min^{-1}, 500 minutes; (D) 0.02 mL min^{-1}, 1000 minutes. Error bars based on propagation of LSC uncertainties

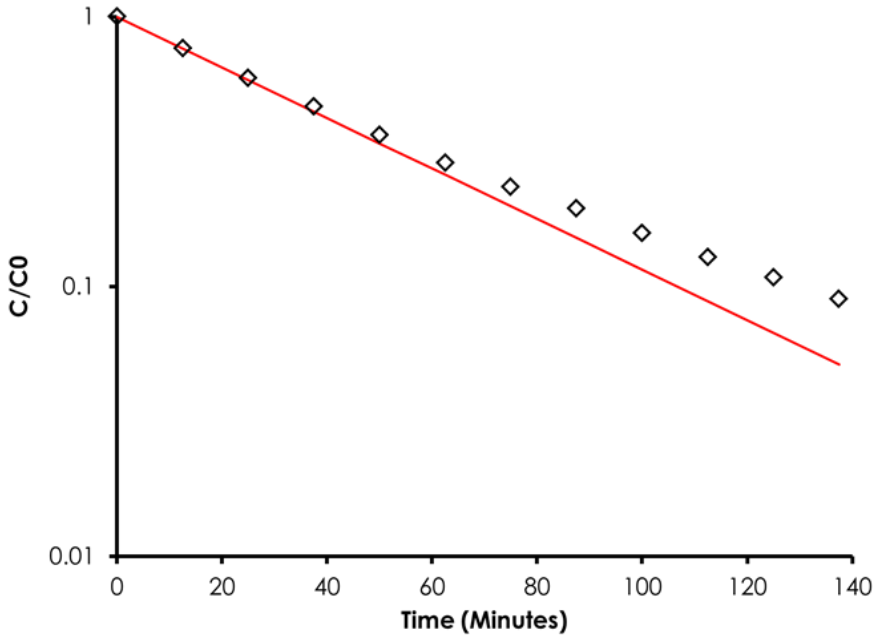

Figure 10 Comparison of expected effluent concentration of a theoretical non-reactive tracer (red line) versus measured effluent concentration of Pu in bentonite flow cell experiment.

Changes in flow rate were made to increase the solution residence time in the flow cell and are denoted by dashed lines in Figure 9. The first flow rate change was from 0.4 mL min^{-1} to 0.2 mL min^{-1} and increased the solution residence time from 50 minutes to 100 minutes. A significant increase in effluent Pu concentration was observed following the change in flow rate, indicating that Pu desorption was rate-limited within the 50 minute residence time (Figure 9). Changing the flow rate from 0.2 mL min^{-1} (100 minute residence) to 0.04 mL min^{-1} (500 minute residence time) also led to a rise in Pu concentration. A further rise in concentration was also observed when the flow rate was decreased from 0.04 mL min^{-1} (500 minute residence time) to 0.02 mL min^{-1} (1000 minute residence time). This last increase in Pu concentration indicates that desorption remains rate limited even at a residence time of 500 minutes (0.35 d). Current efforts are focused on numerically modeling the flow cell data to determine Pu-bentonite sorption/desorption rates. The multi-component model is based on first order reaction equations and was developed to simulate the known Pu redox transformations occurring on the surface of minerals and quantify the various Pu adsorption, desorption, and redox transformation reactions.

The data in Figure 9 are replotted in terms of the cumulative fraction of Pu desorbed from bentonite in Figure 11. Also included in this plot is the data from a parallel experiment at pH 8 performed with montmorillonite. Both the shape of the plots and the final amounts of Pu desorbed are very similar for the two clays, given the initial problem with the stir bar in the bentonite experiment. This behavior is not unexpected in the context of the similarity of Pu adsorption behavior between bentonite and montmorillonite. This plot further demonstrates that it is likely that the montmorillonite component of the bentoniteis controlling the desorption kinetics behavior of Pu associated with bentonite.

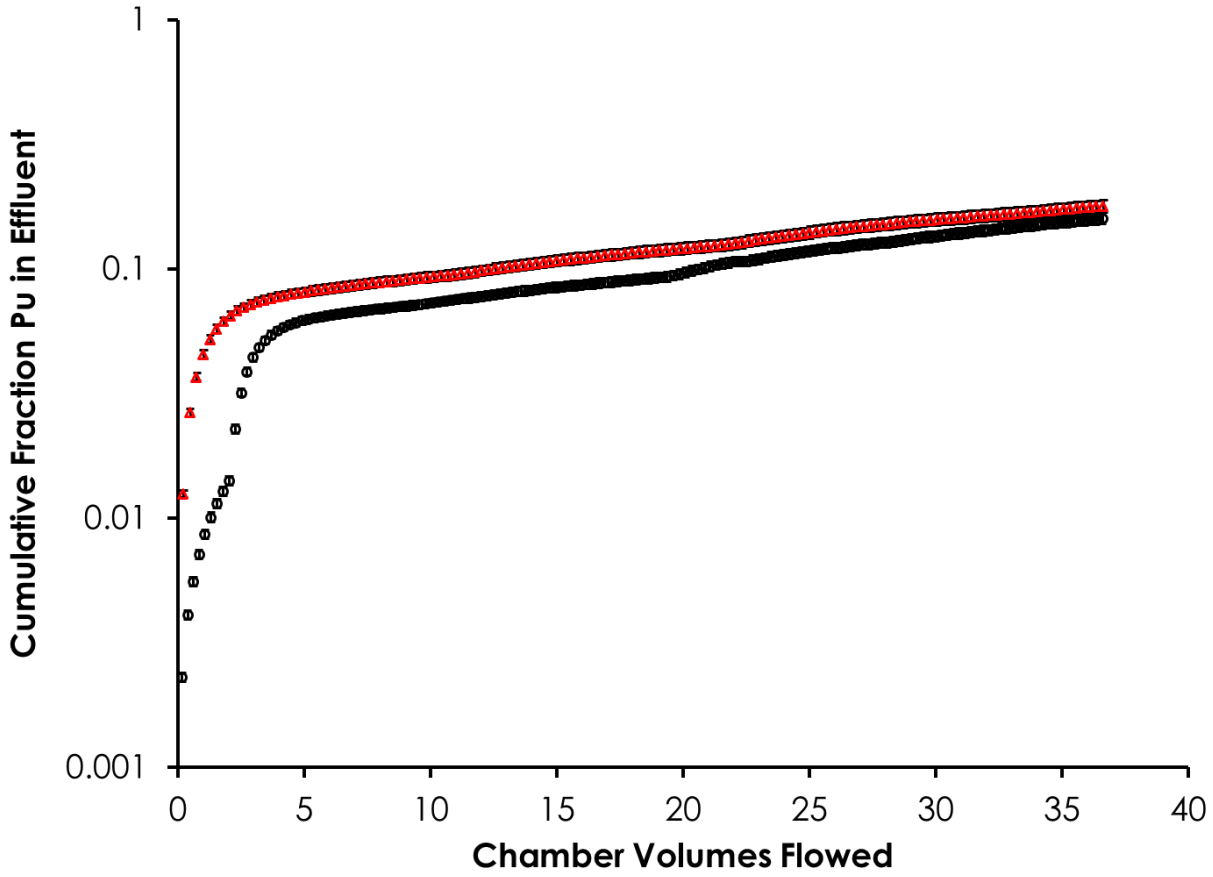

Figure 11. Cumulative fraction of Pu removed from bentonite (black circles) and montmorillonite (red triangles) flow cell experiments. Error bars based on propagation of LSC uncertainties

Based on the Pu concentration at the end of the flow cell experiment, accounting for the net removal of 16.5 % of the Pu from the system (Figure 11), and assuming no change in solid: solution ratio, the calculated apparent log Kd at the end of the flow cell experiment was 6.0 mL g^{-1}. At the end of the flow cell experiment, the Pu-bentonite suspension was allowed to equilibrate under no-flow conditions (0.0 mL min^{-1}). After 60 days, the log K_d was calculated to be 4.8 mL g^{-1} which is in good agreement with K_d values in the Pu(IV) adsorption experiments (4.3 – 4.9 mL/g). The similarity between the adsorption and 2 month desorption K_d values indicates Pu-bentonite sorption reversibility over extended time periods. The slow desorption kinetics observed here highlight why both desorption rates and desorption equilibrium conditions need to be considered when predicting Pu desorption in environmental settings. The slow approach to desorption in these experiments (i.e. on timescales greater than 1 d) is consistent with previous work looking at Pu desorption from montmorillonite, bentonite colloids and argillites.(Huber et al., 2011; Latrille et al., 2006; Lu et al., 2003)

Oxidation state analysis using LaF_3 precipitation was performed on flow cell effluent following the rate change from 0.2 mL min^{-1} to 0.04 mL min^{-1}. The analysis indicated that the desorbed Pu was predominantly in the Pu(V)/(VI) oxidation state (90±10%). This would suggest that in the short term, desorption of Pu(IV) from the mineral surface is driven by oxidation of surface Pu(IV) to Pu(V) which is more readily desorbed. However we cannot verify this without direct oxidation

state analysis of Pu on the mineral surface. Interestingly, oxidation state analysis of the Pu supernatant after the 2 month post flow cell equilibration period indicated that the aqueous Pu was predominantly Pu(IV). This suggests that differences in Pu oxidation state may be responsible for differences in short term and long term desorption behavior of Pu from bentonite.

4. Environmental Implications

Previously, we examined the adsorption of Pu(V) to SWy-1 Na-montmorillonite over a concentration range 10^{-6} – 10^{-16} M to determine if Pu adsorption behavior at concentrations used in typical lab experiments (>10^{-10} M) was comparable to typical environmental concentrations (<10^{-12}M).(Begg et al., 2013) In the current study, we investigated the sorption behavior of less soluble Pu(IV) to FEBEX bentonite over the concentration range 10^{-7} – 10^{-16} M . The results suggest that on the timescale of months, Pu(IV) adsorption affinity for bentonite will be independent of Pu concentration. The adsorption of Pu(IV) to bentonite was very similar to that previously observed for adsorption to colloidal montmorillonite. Experiments with Pu(V) showed that at timescales of several months Pu(V) and Pu(IV) adsorption behavior on bentonite is convergent, highlighting the importance of considering slow adsorption and redox processes when predicting Pu migration in clay environments.

A Pu(IV)-bentonite flow-cell experiment demonstrated the difference in desorption behavior of Pu at a timescale of days compared to months. The kinetics of desorption will be of key importance for predicting the mobility of Pu in groundwater environments, especially if Pu is associated with colloidal phases. Pu oxidation state changes appeared to be linked to the differences in desorption behavior observed at short and long timescales. The desorption of Pu(IV) from bentonite at pH 8 was very similar to that observed for Pu(IV) desorption from SWy-1 montmorillonite. Taken in conjunction with the similarity in adsorption between the two clays, this indicates that montmorillonite controls Pu adsorption in bentonite. Thus we would suggest that the results of Pu adsorption/desorption experiments with SWy-1 could feasibly be used as analogues for FEBEX bentonite behavior.

5. Planned FY15 Efforts

The FY15 effort builds on FY14 experiments in which we examined desorption of Pu from montmorillonite and bentonite. Numerical models were developed that captured Pu redox transformations and sorption/desorption kinetics. Due to its swelling properties, plasticity, ion exchange, sorption and sealing capability, bentonite is a good candidate for backfill material proposed to be used in nuclear waste repository scenarios.(Guven, 1990) However, one of the concerns with the use of bentonite as a backfill material is that it can form colloidal particles which may enhance the migration of radionuclide species.(Geckeis et al., 2004; Kersting et al., 1999) As a result, radionuclide (including Pu) adsorption to mineral colloids has been the subject of considerable study. In contrast, desorption reactions have been far less well studied. This is problematic because application of thermodynamic equilibrium parameters in field transport models which incorrectly represent desorption processes are likely to be flawed.(Artinger et al., 2002)

Recently, we have developed a numerical model to describe the adsorption and desorption behavior of Pu with montmorillonite (a primary constituent of bentonite) colloids.(Begg et al., In Prep) To further test the assumptions in our approach, we propose to apply this numerical model

to data generated in recent Pu-colloid transport experiments performed at the Grimsel Test Site. Comparison of the model and observed behavior will allow us to verify the applicability of our model in field-scale conditions or will otherwise highlight areas of weakness in our understanding of Pu adsorption/desorption mechanisms

6. Acknowledgments

We thank P. Reimus (LANL) for providing the bentonite used in this work. This work was supported by the Used Fuel Disposition Campaign of the Department of Energy's Nuclear Energy Program and the Subsurface Biogeochemical Research Program of the U.S. Department of Energy's Office of Biological and Environmental Research. Prepared by LLNL under Contract DE-AC52-07NA27344.

7. References

Artinger, R., Schuessler, W., Schaefer, T., and Kim, J. I., 2002. A kinetic study of Am(III)/humic colloid interactions. *Environ Sci Technol* **36**, 4358-4363.

Begg, J. D., Zavarin, M., and Kersting, A. B., 2014. Plutonium Desorption from Mineral Surfaces at Environmental Concentrations of Hydrogen Peroxide. *Environ Sci Technol*.

Begg, J. D., Zavarin, M., Zhao, P., Tumey, S. J., Powell, B., and Kersting, A. B., 2013. Pu(V) and Pu(IV) sorption to montmorillonite. *Environ Sci Technol* **47**, 5146-5153.

Begg, J. D. C., Zavarin, M., and Kersting, A., In Prep. Desorption of plutonium from montmorillonite: An experimental and modeling study.

Choppin, G. R., 1991. Redox speciation of plutonium in natural waters. *J Radioan Nucl Ch Ar* **147**, 109-116.

Choppin, G. R., 2007. Actinide speciation in the environment. *J Radioanal Nucl Ch* **273**, 695-703.

Dai, M. H., Buesseler, K., and Pike, S. M., 2005. Plutonium in groundwater at the 100K-Area of the US DOE Hanford site. *Journal of Contaminant Hydrology* **76**, 167-189.

Dozol, M., Hagemann, R., Hoffman, D. C., Adloff, J. P., Vongunten, H. R., Foos, J., Kasprzak, K. S., Liu, Y. F., Zvara, I., Ache, H. J., Das, H. A., Hagemann, R. J. C., Herrmann, G., Karol, P., Maenhaut, W., Nakahara, H., Sakanoue, M., Tetlow, J. A., Baro, G. B., Fardy, J. J., Benes, P., Roessler, K., Roth, E., Burger, K., Steinnes, E., Kostanski, M. J., Peisach, M., Liljenzin, J. O., Aras, N. K., Myasoedov, B. F., and Holden, N. E., 1993. Radionuclide migration in groundwaters - Review of the behavior of actinides (Technical report) *Pure and Applied Chemistry* **65**, 1081-1102.

Efurd, D. W., Runde, W., Banar, J. C., Janecky, D. R., Kaszuba, J. P., Palmer, P. D., Roensch, F. R., and Tait, C. D., 1998. Neptunium and plutonium solubilities in a Yucca Mountain groundwater. *Environ Sci Technol* **32**, 3893-3900.

Fernandez, A. M., Baeyens, B., Bradbury, M., and Rivas, P., 2004. Analysis of the porewater chemical composition of a Spanish compacted bentonite used in an engineered barrier. *Physics and Chemistry of the Earth* **29**, 105-118.

Geckeis, H., Schafer, T., Hauser, W., Rabung, T., Missana, T., Degueldre, C., Mori, A., Eikenberg, J., Fierz, T., and Alexander, W. R., 2004. Results of the colloid and radionuclide retention experiment (CRR) at the Grimsel Test Site (GTS), Switzerland - impact of reaction kinetics and speciation on radionuclide migration. *Radiochim Acta* **92**, 765-774.

Grauer, R., 1986. Bentonite as a backfill material in the high-level waste repository: Chemical aspects*EIR Bericht Nr. 576, Nagra Technical Report NTB 86-12E*. Paul Scherrer Institut, Villigen, Switzerland and Nagra, Wettingen, Switzerland.

Grim, R. E., 1968. *Clay mineralogy*. McGraw Hill.

Guillaumont, R., Fanghanel, T., Neck, V., Fuger, J., Palmer, D. A., Grenthe, I., and Rand, M. H., 2003. Update on the chemical thermodynamics of uranium, neptunium, plutonium, americium, and technetium. In: Mompean, F. J., Illemassene, M., Domenech-Orti, C., and Said, K. B. Eds.)*Chemical Thermodynamics*. Elsevier, Amsterdam.

Guven, N., 1988. Smectites. *Reviews in Mineralogy and Geochemistry* **19**, 497-559.

Guven, N., 1990. Longevity of bentonite as buffer material in a nuclear-waste repository. *Engineering Geology* **28**, 233-247.

Huber, F., Kunze, P., Geckeis, H., and Schafer, T., 2011. Sorption reversibility kinetics in the ternary system radionuclide-bentonite colloids/nanoparticles-granite fracture filling material. *Appl. Geochem.* **26**, 2226-2237.

IAEA, 1995. Principles of Radioactive Waste Management*Safety Series* IAEA, Vienna.

Icopini, G. A., Lack, J. G., Hersman, L. E., Neu, M. P., and Boukhalfa, H., 2009. Plutonium(V/VI) reduction by the metal-reducing Bacteria Geobacter metallireducens GS-15 and Shewanella oneidensis MR-1. *Appl. Environ. Microbiol.* **75**, 3641-3647.

Kaplan, D. I., Powell, B. A., Duff, M. C., Demirkanli, D. I., Denham, M., Fjeld, R. A., and Molz, F. J., 2007. Influence of sources on plutonium mobility and oxidation state transformations in vadose zone sediments. *Environ Sci Technol* **41**, 7417-7423.

Keeney-Kennicutt, W. L. and Morse, J. W., 1985. The redox chemistry of $Pu(V)O_2^+$ interaction with common mineral surfaces in dilute solutions and seawater. *Geochim Cosmochim Ac* **49**, 2577-2588.

Kersting, A. B., Efurd, D. W., Finnegan, D. L., Rokop, D. J., Smith, D. K., and Thompson, J. L., 1999. Migration of plutonium in ground water at the Nevada Test Site. *Nature* **397**, 56-59.

Kobashi, A. and Choppin, G. R., 1988. A study of techniques for separating plutonium in different oxidation states. *Radiochim. Acta* **43**, 211-215.

Latrille, C., Ly, J., and Herbette, M., 2006. Retention of Sn(IV) and Pu(IV) onto four argillites from the Callovo-Oxfordian level at Bure (France) from eight equilibrated sedimentary waters. *Radiochim Acta* **94**, 421-427.

Lu, N. P., Reimus, P. W., Parker, G. R., Conca, J. L., and Triay, I. R., 2003. Sorption kinetics and impact of temperature, ionic strength and colloid concentration on the adsorption of plutonium-239 by inorganic colloids. *Radiochim Acta* **91**, 713-720.

Lujaniene, G., Motiejunas, S., and Sapolaite, J., 2007. Sorption of Cs, Pu and Am on clay minerals. *J Radioanal Nucl Ch* **274**, 345-353.

Marchetti, A. A., Brown, T. A., Cox, C. C., Hamilton, T. F., and Martinelli, R. E., 2005. Accelerator mass spectrometry of actinides. *J Radioanal Nucl Ch* **263**, 483-487.

McCubbin, D. and Leonard, K. S., 1996. Photochemical dissolution of radionuclides from marine sediments. *Mar Chem* **55**, 399-408.

Missana, T., Alonso, U., Garcia-Gutierrez, M., and Mingarro, M., 2008. Role of bentonite colloids on europium and plutonium migration in a granite fracture. *Appl. Geochem.* **23**, 1484-1497.

Missana, T. and Garcia-Gutierrez, M., 2007. Adsorption of bivalent ions (Ca(II), Sr(II) and Co(II)) onto FEBEX bentonite. *Physics and Chemistry of the Earth* **32**, 559-567.

Missana, T., Garcia-Gutierrez, M., and Alonso, U., 2004. Kinetics and irreversibility of cesium and uranium sorption onto bentonite colloids in a deep granitic environment. *Applied Clay Science* **26**, 137-150.

NAGRA, 2006. The CRR Final Project Report Series II: Supporting Laboratory Experiments with Radionuclides and Bentonite Colloids. Technical Report 03-02. In: Missana, T. and Geckeis, H. Eds.). Nagra, Wettingen, Switzerland

Neck, V., Altmaier, M., and Fanghanel, T., 2007a. Solubility of plutonium hydroxides/hydrous oxides under reducing conditions and in the presence of oxygen. *Comptes Rendus Chimie* **10**, 959-977.

Neck, V., Altmaier, M., Seibert, A., Yun, J. I., Marquardt, C. M., and Fanghanel, T., 2007b. Solubility and redox reactions of Pu(IV) hydrous oxide: Evidence for the formation of $PuO_{2+x(s, hyd)}$. *Radiochim Acta* **95**, 193-207.

Nitsche, H. and Edelstein, N. M., 1985. Solubilities and speciation of selected transuranium ions. A comparison of a non-complexing solution with a groundwater from the Nevada Tuff Site. *Radiochim Acta* **39**, 23-33.

Novikov, A. P., Kalmykov, S. N., Utsunomiya, S., Ewing, R. C., Horreard, F., Merkulov, A., Clark, S. B., Tkachev, V. V., and Myasoedov, B. F., 2006. Colloid transport of plutonium in the far-field of the Mayak Production Association, Russia. *Science* **314**, 638-641.

Orlandini, K. A., Penrose, W. R., and Nelson, D. M., 1986. Pu(V) as the stable form of oxidized plutonium in natural waters. *Mar Chem* **18**, 49-57.

Penrose, W. R., Polzer, W. L., Essington, E. H., Nelson, D. M., and Orlandini, K. A., 1990. MOBILITY OF PLUTONIUM AND AMERICIUM THROUGH A SHALLOW AQUIFER IN A SEMIARID REGION. *Environ Sci Technol* **24**, 228-234.

Powell, B. A., Dai, Z. R., Zavarin, M., Zhao, P. H., and Kersting, A. B., 2011. Stabilization of plutonium nano-colloids by epitaxial distortion on mineral surfaces. *Environ Sci Technol* **45**, 2698-2703.

Powell, B. A., Fjeld, R. A., Kaplan, D. I., Coates, J. T., and Serkiz, S. M., 2004. $Pu(V)O_2^+$ adsorption and reduction by synthetic magnetite (Fe_3O_4). *Environ Sci Technol* **38**, 6016-6024.

Powell, B. A., Fjeld, R. A., Kaplan, D. I., Coates, J. T., and Serkiz, S. M., 2005. $Pu(V)O_2^+$ adsorption and reduction by synthetic hematite and goethite. *Environ Sci Technol* **39**, 2107-2114.

Romanchuk, A. Y., Kalmykov, S. N., and Aliev, R. A., 2011. Plutonium sorption onto hematite colloids at femto- and nanomolar concentrations. *Radiochim Acta* **99**, 137-144.

Ross, C. S. and Shannon, E. V., 1926. The minerals of bentonite and related clays and their physical properties. *Journal of the American Ceramic Society* **9**, 77-96.

Runde, W., Conradson, S. D., Efurd, D. W., Lu, N. P., VanPelt, C. E., and Tait, C. D., 2002. Solubility and sorption of redox-sensitive radionuclides (Np, Pu) in J-13 water from the Yucca Mountain site: comparison between experiment and theory. *Appl. Geochem.* **17**, 837-853.

Sabodina, M. N., Kalmykov, S. N., Sapozhnikov, Y. A., and Zakharova, E. V., 2006. Neptunium, plutonium and ^{137}Cs sorption by bentonite clays and their speciation in pore waters. *J Radioanal Nucl Ch* **270**, 349-355.

Sanchez, A. L., Murray, J. W., and Sibley, T. H., 1985. The adsorption of plutonium IV and plutonium V on goethite. *Geochim Cosmochim Ac* **49**, 2297-2307.

Santschi, P. H., Roberts, K. A., and Guo, L. D., 2002. Organic nature of colloidal actinides transported in surface water environments. *Environ Sci Technol* **36**, 3711-3719.

Schwenk-Ferrero, A., 2013. German spent nuclear fuel legacy: Characteristics and high-level waste management issues. *Science and Technology of Nuclear Installations* **2013**, 11.

Silva, R. J. and Nitsche, H., 1995. Actinide environmental chemistry. *Radiochim Acta* **70-1**, 377-396.

Snow, M. S., Zhao, P. H., Dai, Z. R., Kersting, A. B., and Zavarin, M., 2013. Neptunium(V) sorption to goethite at attomolar to micromolar concentrations using radiometric methods. *Journal of Colloid and Interface Science* **390**, 176-182.

Tinnacher, R. M., Zavarin, M., Powell, B. A., and Kersting, A. B., 2011. Kinetics of neptunium(V) sorption and desorption on goethite: An experimental and modeling study. *Geochim Cosmochim Ac* **75**, 6584-6599.

Vaniman, D., Furlano, A., Chipera, S., Thompson, J., and Triay, I., 1995. Microautoradiography in studies of Pu(V) sorption by trace and fracture minerals in tuff. *MRS Proceedings* **412**, 639-646.

Zavarin, M., Powell, B. A., Bourbin, M., Zhao, P. H., and Kersting, A. B., 2012. Np(V) and Pu(V) ion exchange and surface-mediated reduction mechanisms on montmorillonite. *Environ Sci Technol* **46**, 2692-2698.

Zhao, P. H., Zavarin, M., Leif, R. N., Powell, B. A., Singleton, M. J., Lindvall, R. E., and Kersting, A. B., 2011. Mobilization of actinides by dissolved organic compounds at the Nevada Test Site. *Appl. Geochem.* **26**, 308-318.